Supplementary Material

Enhancing Inflammation Targeting Using Tunable Leukocyte-Based Biomimetic Nanoparticles

Assaf Zinger[1,2,†,*], Manuela Sushnitha[1,2,3,†], Tomoyuki Naoi[1,2], Gherardo Baudo[1,2], Enrica De Rosa[1,2], Jenny Chang[4], Ennio Tasciotti[1,2,5] and Francesca Taraballi[1,2,*]

[1]Center for Musculoskeletal Regeneration, Houston Methodist Academic Institute, Houston, TX 77030, USA
[2]Orthopedics and Sports Medicine, Houston Methodist Hospital, Houston, TX 77030, USA
[3]Department of Bioengineering, Rice University, Houston, Houston, TX 77030, USA
[4]Houston Methodist Cancer Center, Houston Methodist Hospital, Houston, TX 77030, USA
[5]Biotechnology Program, San Raffaele University and IRCCS San Raffaele Pisana, 00166 Roma RM, Italy

† These authors contributed equally to this work

* To whom correspondence should be addressed:

Dr. Francesca Taraballi

Center for Musculoskeletal Regeneration

Houston Methodist Academic Institute

6670 Bertner Ave, Houston, TX, 77030

Tel: +1 713-441-3473

ftaraballi2@houstonmethodist.org

Dr. Assaf Zinger

Center for Musculoskeletal Regeneration

Houston Methodist Academic Institute

6670 Bertner Ave, Houston, TX, 77030

Tel:+1 713-441-7432

ayzinger@houstonmethodist.org

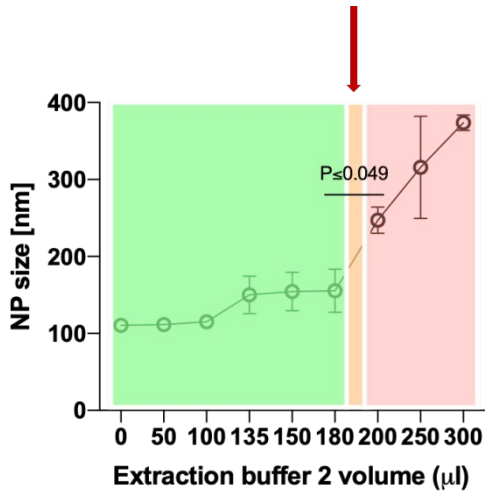

Fig. S1. Effect of protein buffer on NP size

Increasing volume of protein buffer in aqueous phase of the NP synthesis resulted in an associated increase of NP size, with 180uL being the maximum volume to be used in order to maintain a NP size of 200 nm. Results are shown as mean ± SEM, N = 3. Unpaired, two-tailed t-test was used to determine significant difference between 180 µl to 200 µl. A P-value ≤ 0.05 was determined to be significant.

A

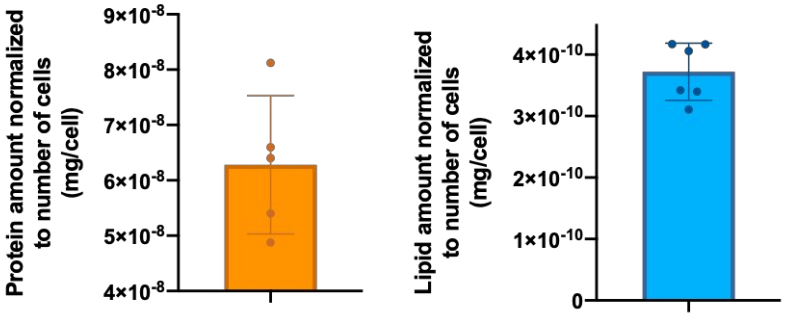

B

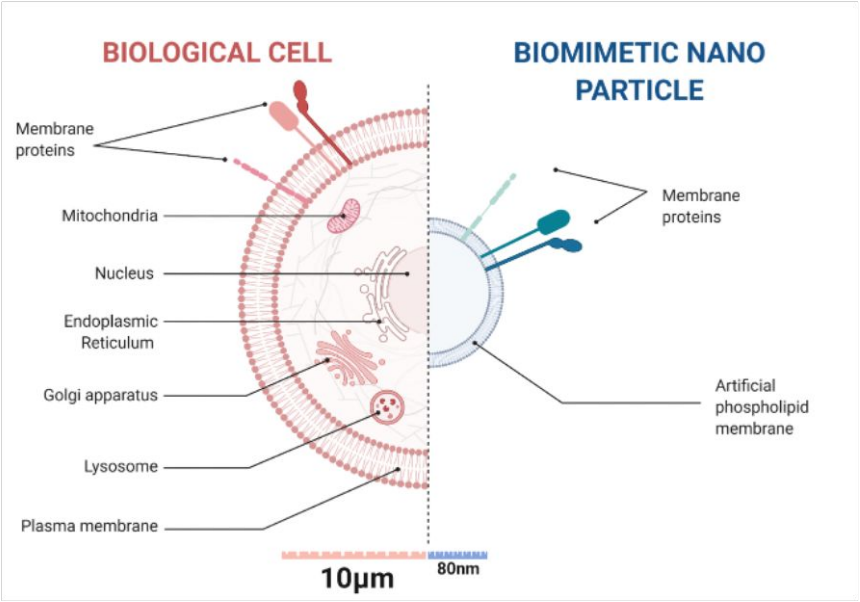

C

Calculated protein:lipid ratio of native cell	168.75
Surface area of cell [A]	1256.64 um^2
Surface area of NP [B]	80424.77 nm^2
Scaling factor [A/B]	15625
Protein:lipid ratio of cell with scaling factor	0.0108

Fig. S2. Native protein:lipid ratio

Combining empirical and mathematical calculations, the native P:L ratio of the cells used to synthesize particles was calculated to be 0.01. A) Quantification of amount of proteins (left) and lipids (right) of J774 cells. B) Schematic highlighting the size and component differences of cells and NP. C) Table outlining the calculated values based on the quantification from (A) and scaling factor calculated based on the surface area of cells and NP.

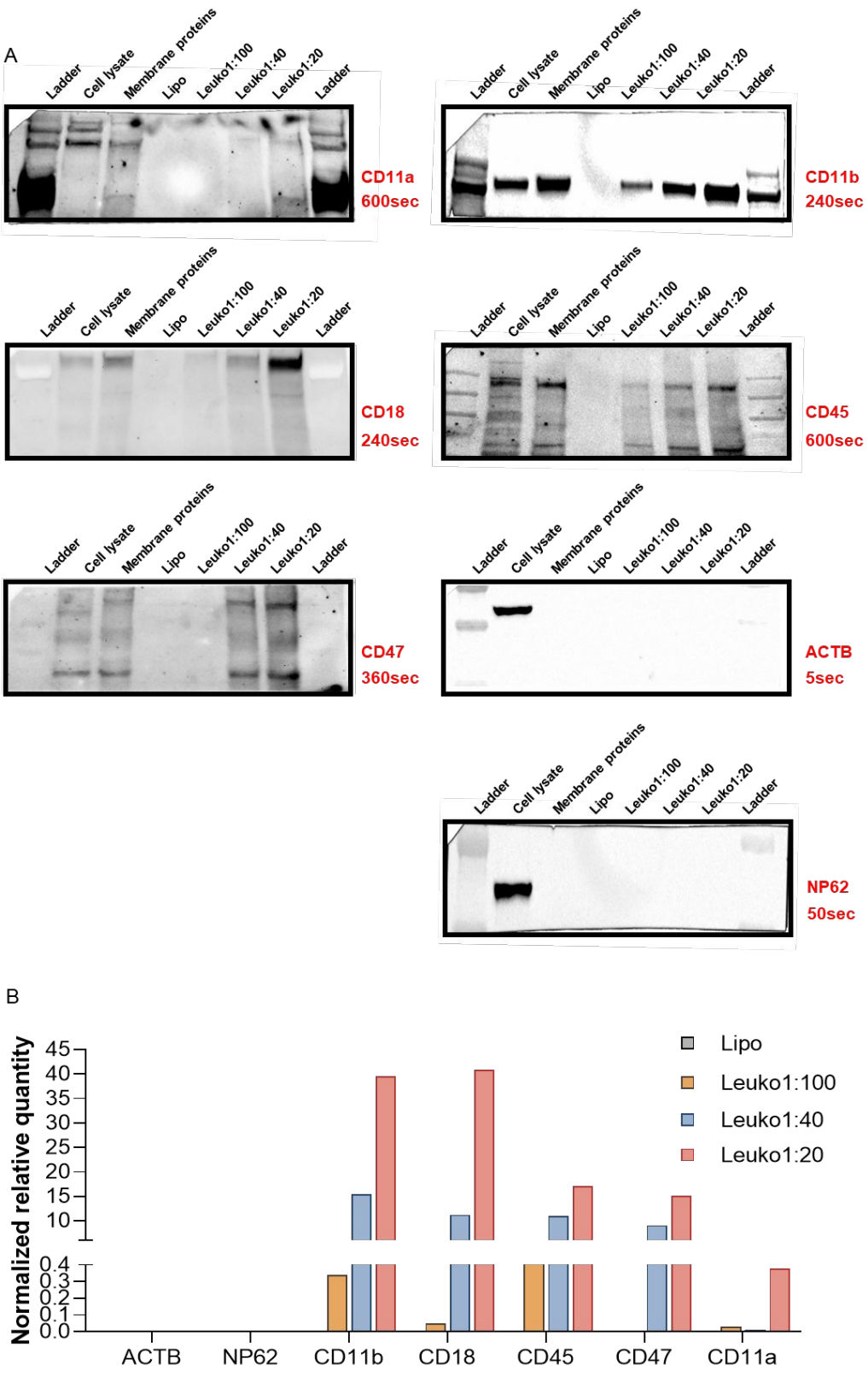

Fig. S3. NP biomimetic markers, original WB membranes and quantification.
Five leukocytes membrane proteins markers and one intracellular marker were characterized and quantified after the NP synthesis and purification (A). WB quantification indicates an increase in CD11a, CD11b, CD18, CD45 and CD47 quantity among the NP groups with no presence of intracellular protein marker, ACTB, or nuclear protein marker, NP62 (B).

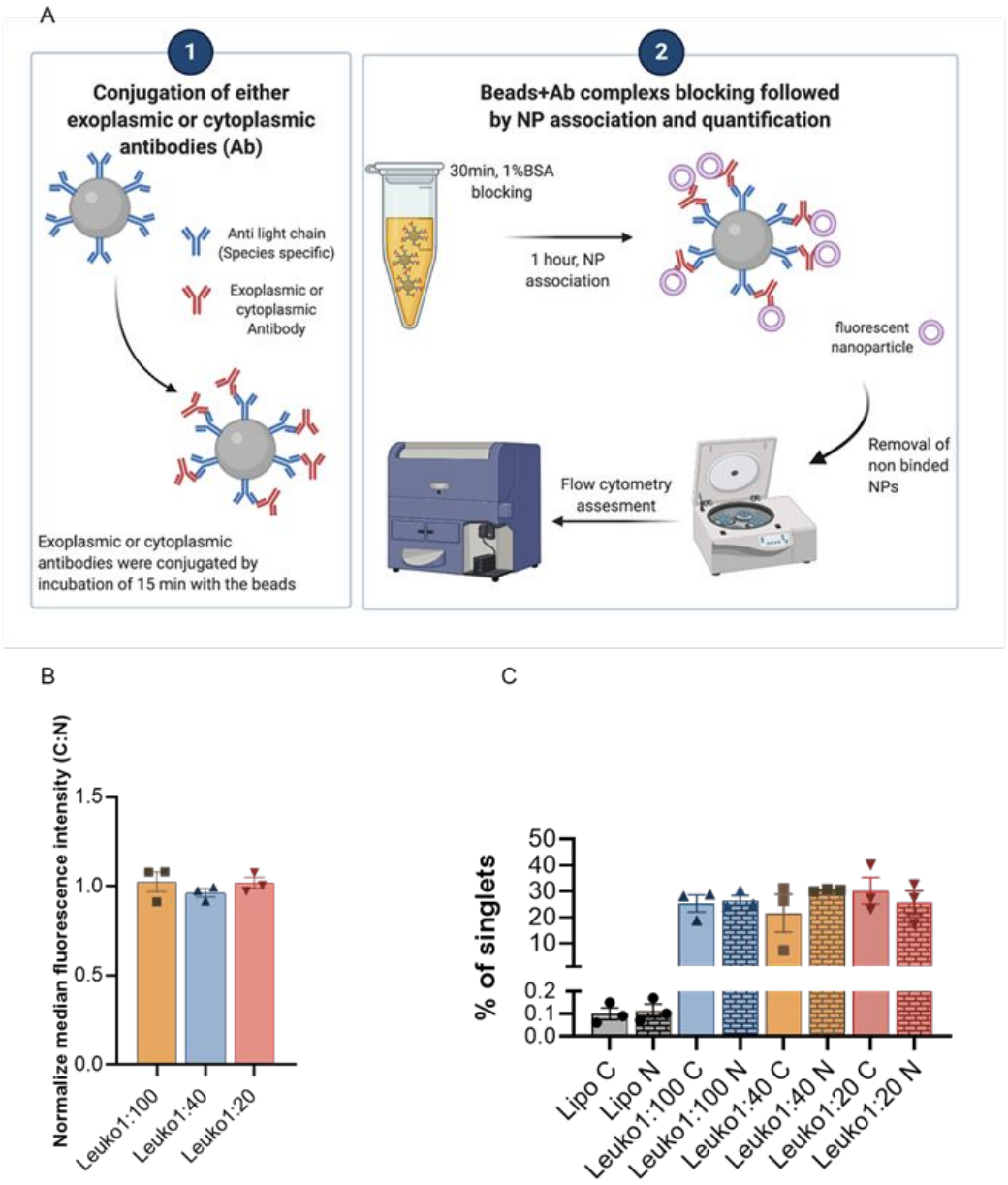

Fig. S4. CD11b orientation studies revealed equal distribution of the cytoplasmic and exoplasmic parts.

(A) CD11b orientation was studied by conjugating either exoplasmic (N) or cytoplasmic (C) antibodies (Ab) to the surface of 2.8µm mice IgG compensation beads. The beads+Ab complex were blocked for 30min at RT using 1% BSA solution to prevent nonspecific binding. Subsequently, fluorescent biomimetic NP were incubated with the beads+Ab complex for 1 hour followed by three times of centrifugation to remove any unreacted Ab. The beads+Ab+fluorescent biomimetic NP were then analyzed using a LSRFortessa cell analyzer to assess the correct membrane protein orientation. (B) Equal distribution between the *C:N terminal* were assessed when we normalized the median florescence intensity of each group. (C) ~25% of singlet gate events were assessed for each of the Leuko groups while only ~0.1% of singlet gate events were assessed for the Lipo group. One-way ANOVA followed by Tukey's multiple comparison test was used to determine statistical probabilities. P value≤0.05 among means was considered as statistically significant. In tile C, all groups of the leukosomes were statistically significant compared to the liposomes group (P value<0.01 at least).

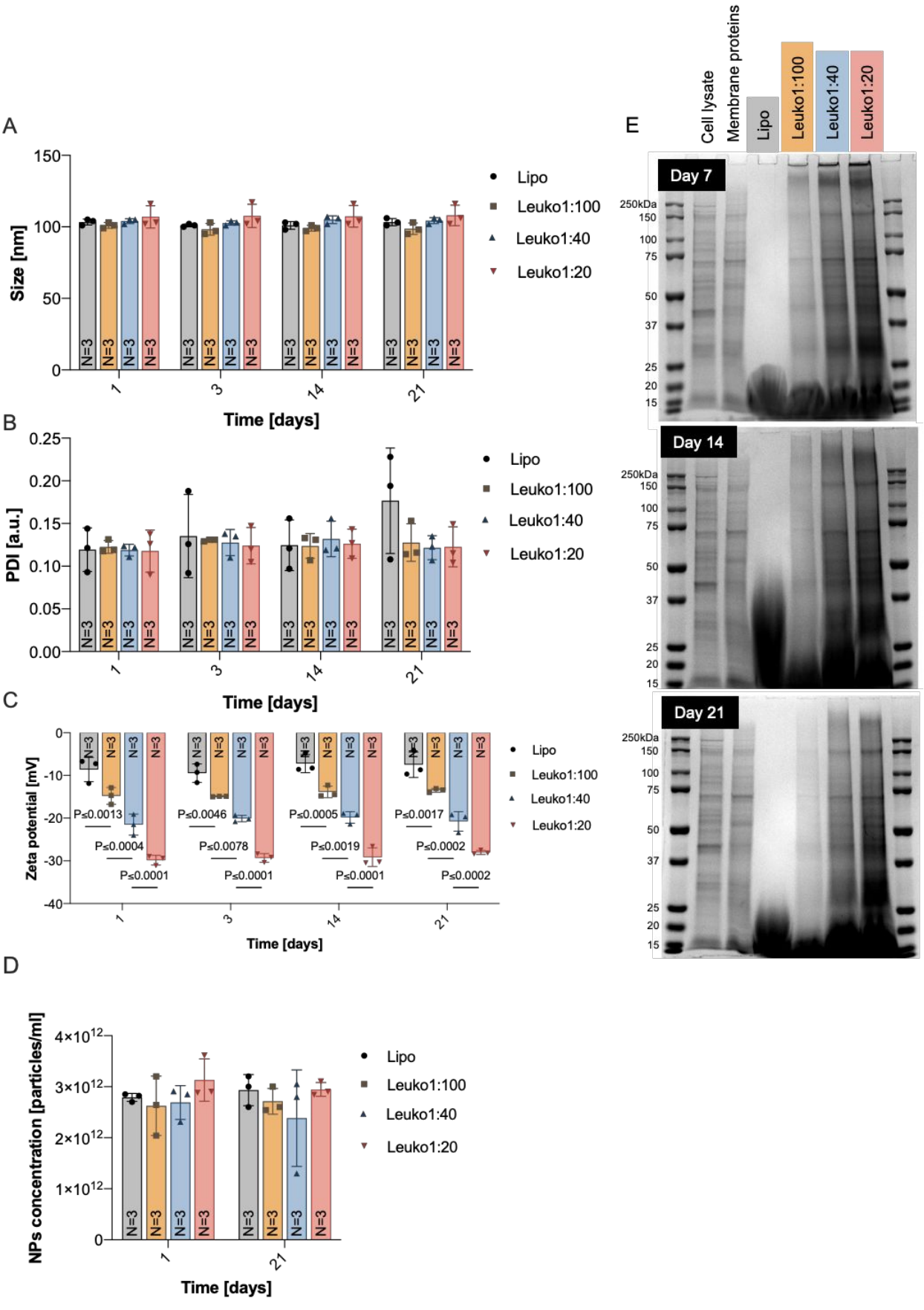
A
Size [nm]
Time [days]
Lipo
Leuko1:100
Leuko1:40
Leuko1:20
B
PDI [a.u.]
Time [days]
C
Zeta potential [mV]
P≤0.0013
P≤0.0004
P≤0.0001
P≤0.0046
P≤0.0078
P≤0.0001
P≤0.0005
P≤0.0019
P≤0.0001
P≤0.0017
P≤0.0002
P≤0.0002
Time [days]
D
NPs concentration [particles/ml]
Time [days]
E
Cell lysate
Membrane proteins
Lipo
Leuko1:100
Leuko1:40
Leuko1:20
Day 7
Day 14
Day 21
250kDa
150
100
75
50
37
25
20
15

Fig. S5. 21-day NP storage stability studies

Physicochemical and biological characterization of NP over 21 days (MilliQ water, 4°C) showed no significant changes in their physicochemical properties while Leuko1:20 maintained a higher protein content. Dynamic light scattering and NanoSight analysis of all NP formulations for (A) size, (B) PDI, (C) zeta potential and (D) concentration (N = 4). SDS-Page gels for protein content on all NP formulations showed higher protein content with increasing protein incorporation on NP (E) (Day 0 SDS gel, (Fig. 2F)). Results are shown as mean ± SEM. Two-way ANOVA followed by Tukey's multiple comparison test was used to determine statistical probabilities. P value≤0.05 among means was considered as statistically significant.

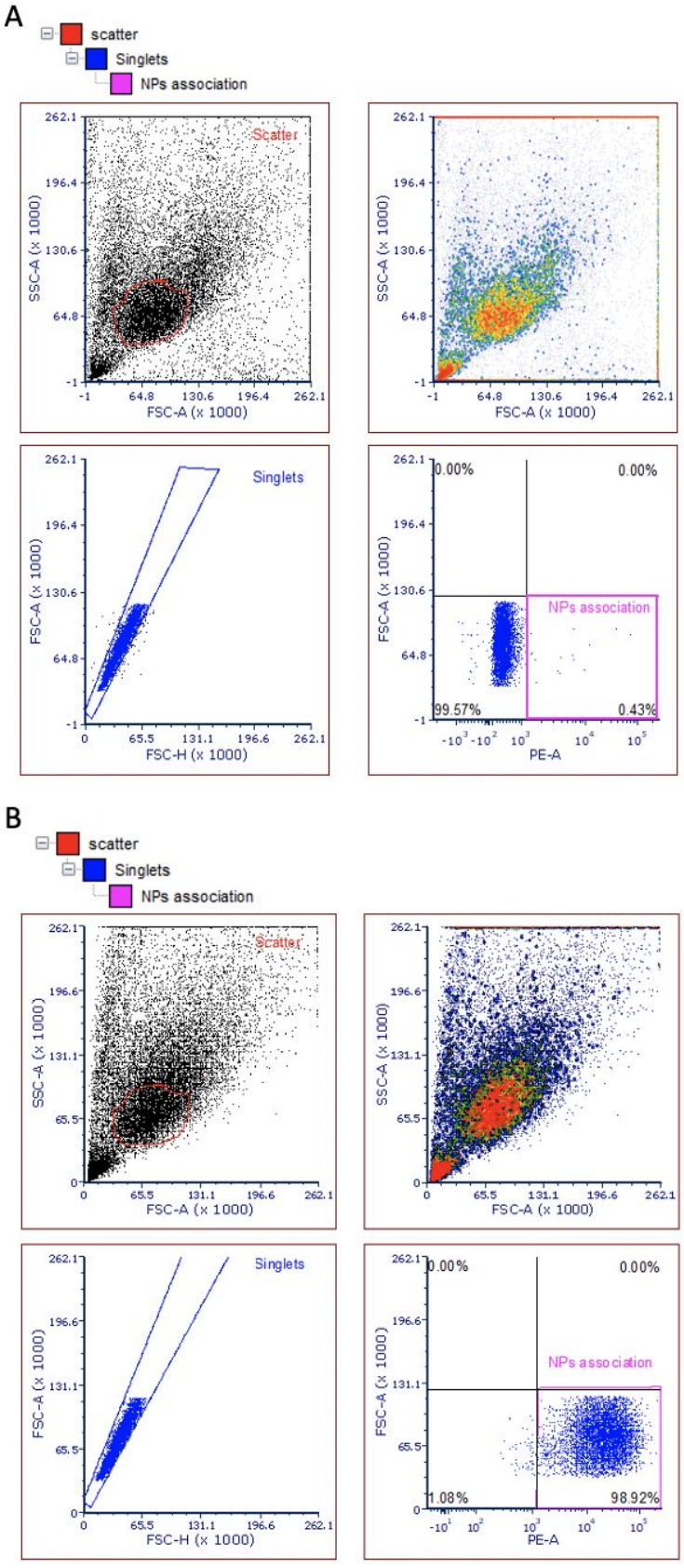

Fig. S6. Gating strategy for flow cytometry analysis of NP uptake
A) Gating for control cells B) Gating for cells treated with biomimetic NP.

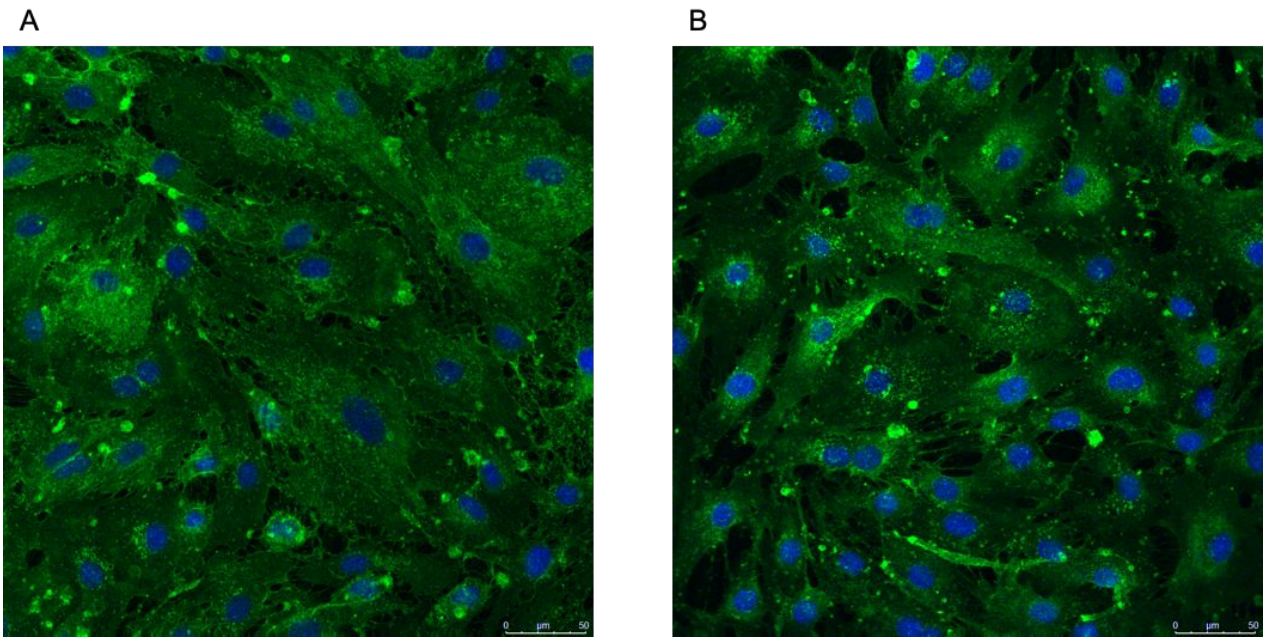

Fig. S7. Non-inflamed and LPS-inflamed endothelial cells.
Non-inflamed (A) and LPS-inflamed (100ng/mL) endothelial cells (B). Scale bars=50µm.

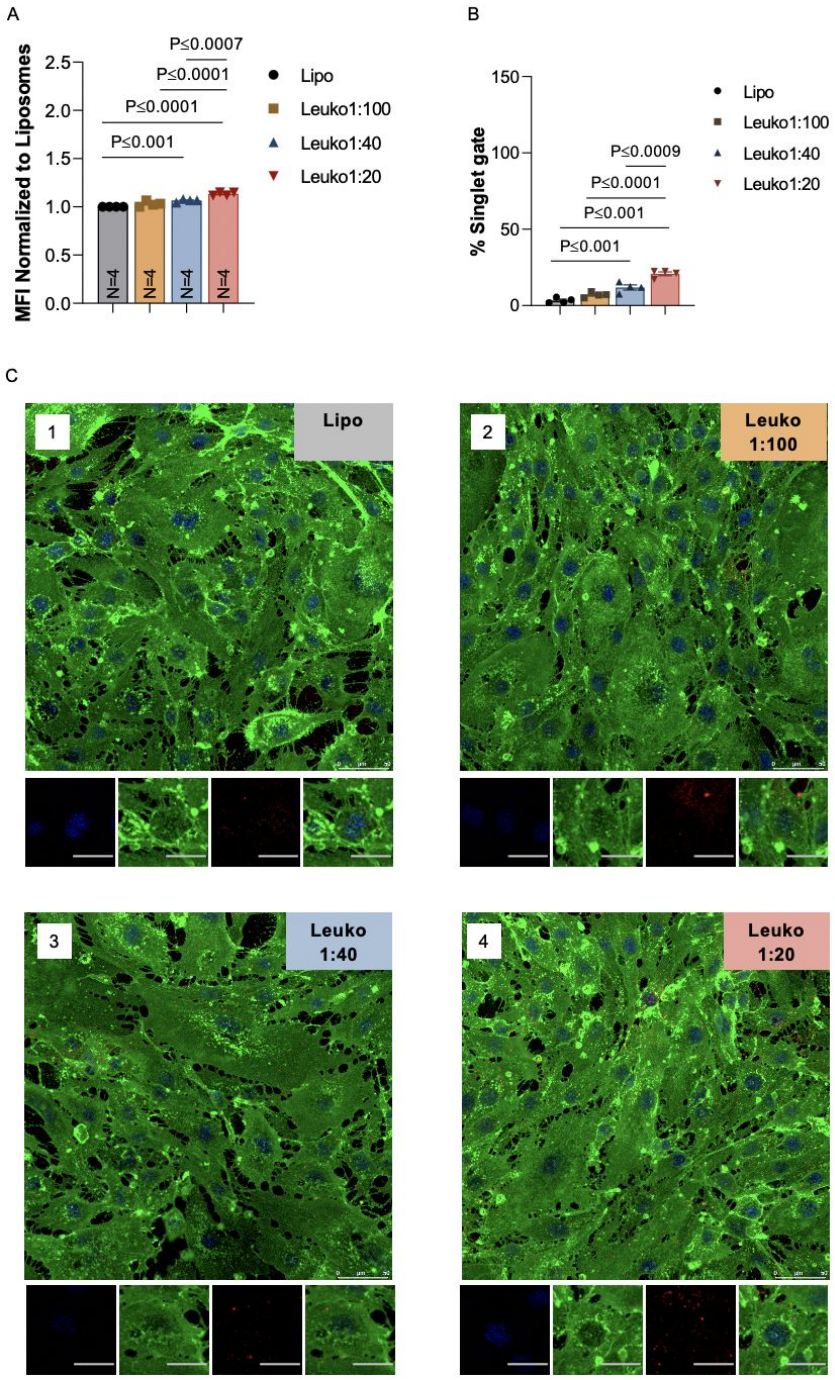

Fig. S8. *In vitro* association and uptake of biomimetic NP by non-inflamed murine endothelial cells

NP association by inflamed endothelial cells was confirmed by flow cytometry (A). Both metrics of relative uptake, as measured by median fluorescence intensity normalized to the liposomes treated cells and % of events from the singlets gate, increased with increasing protein content on NP. Non-inflamed endothelial uptake of fluorescent NP (red) was also visualized by Z-stack confocal imaging (C). Following a 1h incubation, Leuko1:20 demonstrated significantly higher uptake across all NP formulations. Endothelial cells were stained for nuclei (blue) and cell membrane (green). Macro scale bar = 50 µm, micro scale bar = 27 µm. Results are shown as mean ± SEM. Either One-way (A) or two-way (B) ANOVA followed by Tukey's multiple comparison test was used to determine statistical probabilities. P value≤0.05 among means was considered as statistically significant. Confocal images were adjusted by +40% brightness -40% contrast.

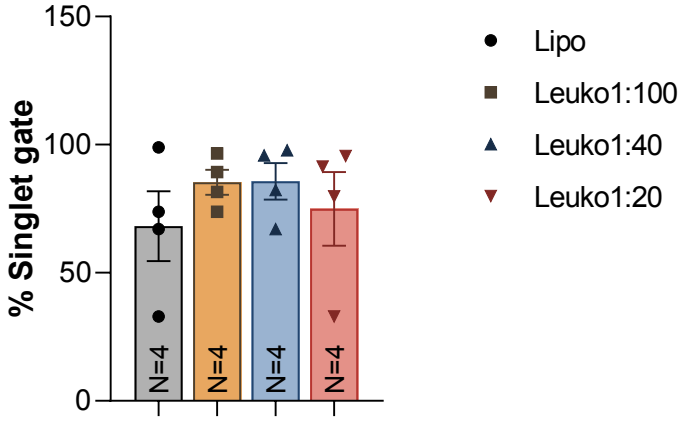

Fig. S9. Percentage of positive cells in singlet gate of inflamed treated cells
The percentage of cells in the positive gate of the singlet gates was quantified. No significant differences were observed across the groups.

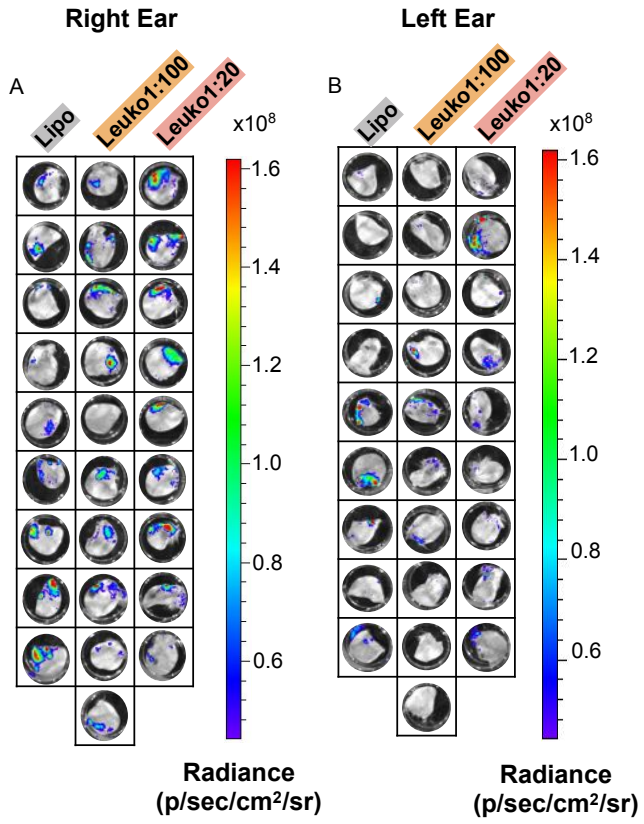

Fig. S10. *Ex vivo* imaging of left and right ears for biomimetic NP targeting in a LLI model. *Ex vivo* imaging of both inflamed right (A) and non-inflamed left (B) ears of the LLI model mice demonstrated NP targeting only in the inflamed, right ears. The low signal detected in the left ears is attributed to the presence of blood in the lower part at site of the cut.

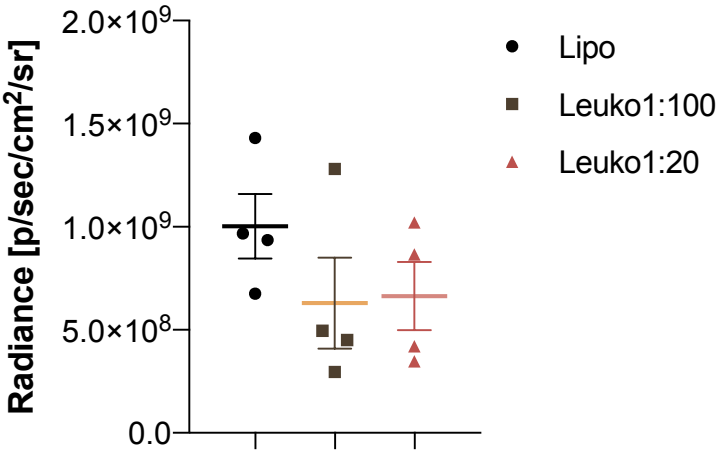

Fig. S11. TNBC tumor luminescence quantification.
Mice were imaged 10 minutes post intraperitoneal injection of luciferin at 150mg/kg. As no statistically significant difference was determined following quantification of the luminescence signal, tumors were deemed to be similar in size prior to administration of NP. Results are shown as mean ± SEM. One-way ANOVA followed by Tukey's multiple comparison test was used to determine statistical probabilities. P value≤0.05 among means was considered as statistically significant.

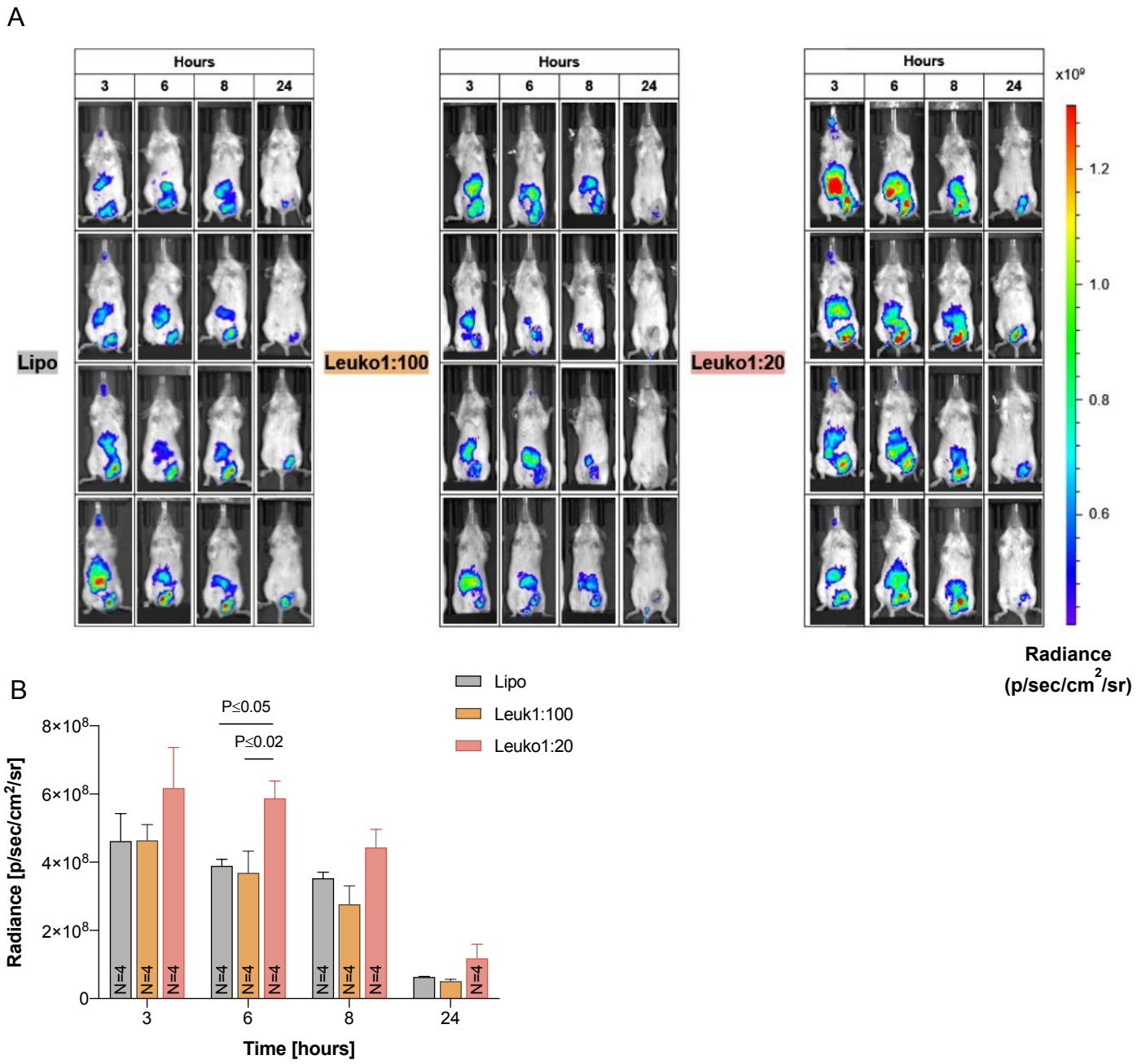

Fig. S12. *In vivo* biomimetic NP liver accumulation in TNBC model.
In vivo images and quantification of NP fluorescence in the livers of TNBC tumor-bearing mice indicated the higher accumulation of Leuko1:20 for up to 8h when compared to the other NP groups. Results are shown as mean ± SEM. Two-way ANOVA followed by Tukey's multiple comparison test was used to determine statistical probabilities. P value≤0.05 among means was considered as statistically significant.

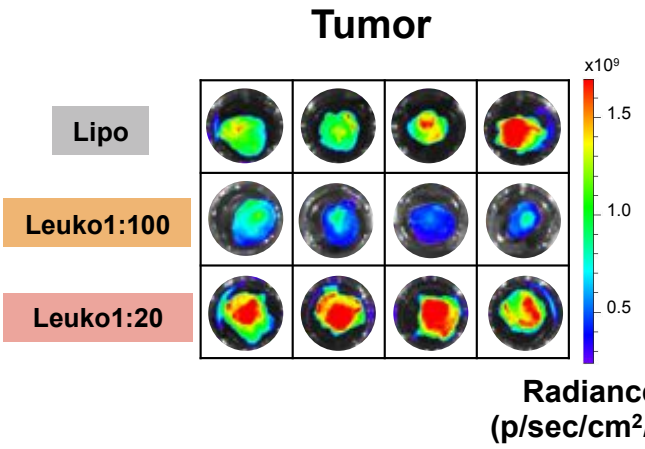

Fig. S13. *Ex vivo* imaging of TNBC tumors for NP accumulation after 24h
IVIS images of TNBC tumors at 24h confirmed the higher NP accumulation of Leuko1:20 when compared to other NP groups.

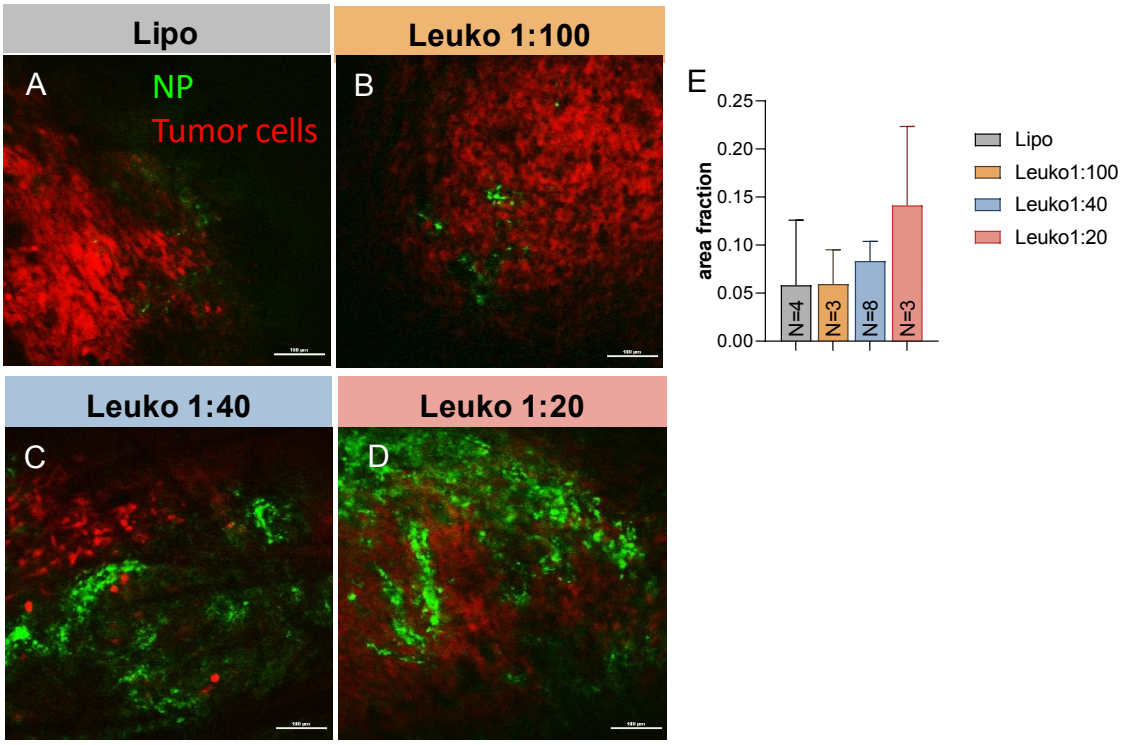

Fig. S14. Intravital microscopy for NP accumulation in inflamed vasculature of TNBC mice
Leuko 1:20 demonstrated higher targeting to the inflamed blood vessels of the tumor 3 hr after systemic administration The NP were imaged and assessed using intravital microscopy. (A) Lipo, (B) Leuko1:100, (C) Leuko1:40, and (D) Leuko1:20. (E) Quantitative analysis of minimum 5 different locations in at least 3 mice for each group of NP. Scale bar = 100 µm. Contrast was adjusted +20% for all images.

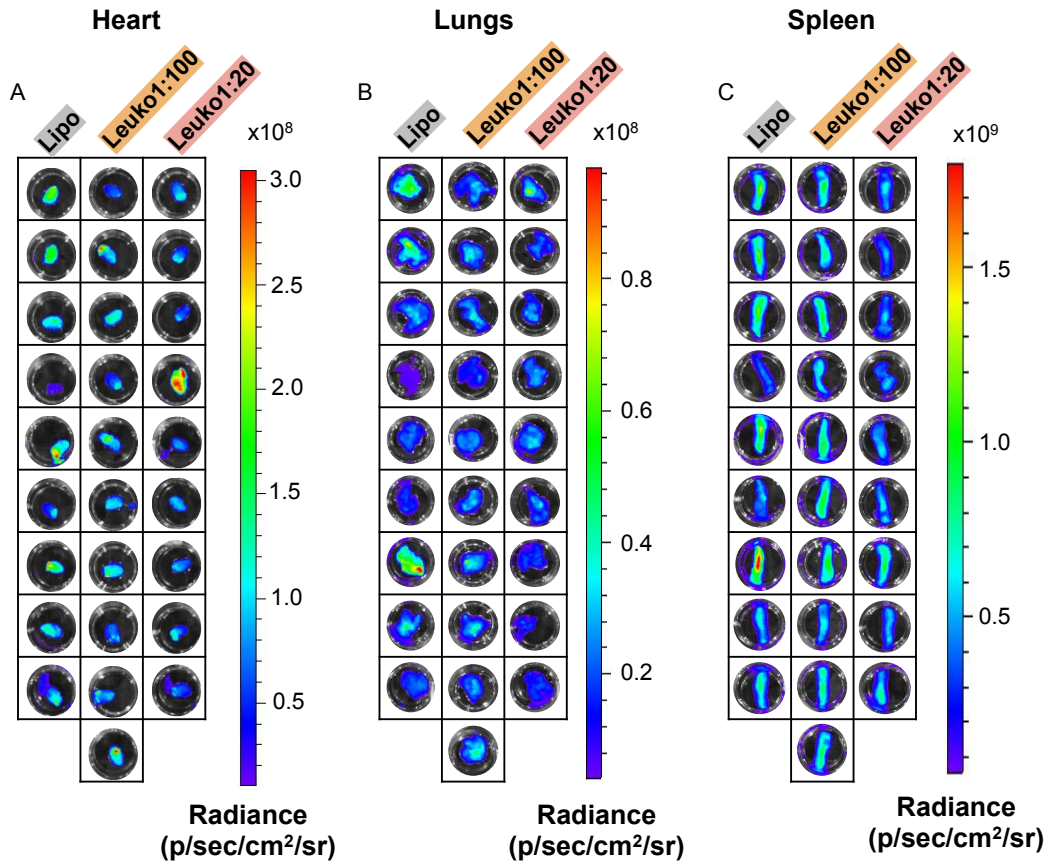

Fig. S15. Biomimetic NP accumulation in heart, lungs and spleen in LLI model after 8h
Ex vivo imaging of heart (A), lungs (B) and spleen (C) of the LLI model mice. No major differences were observed in the NP accumulation in these organs.

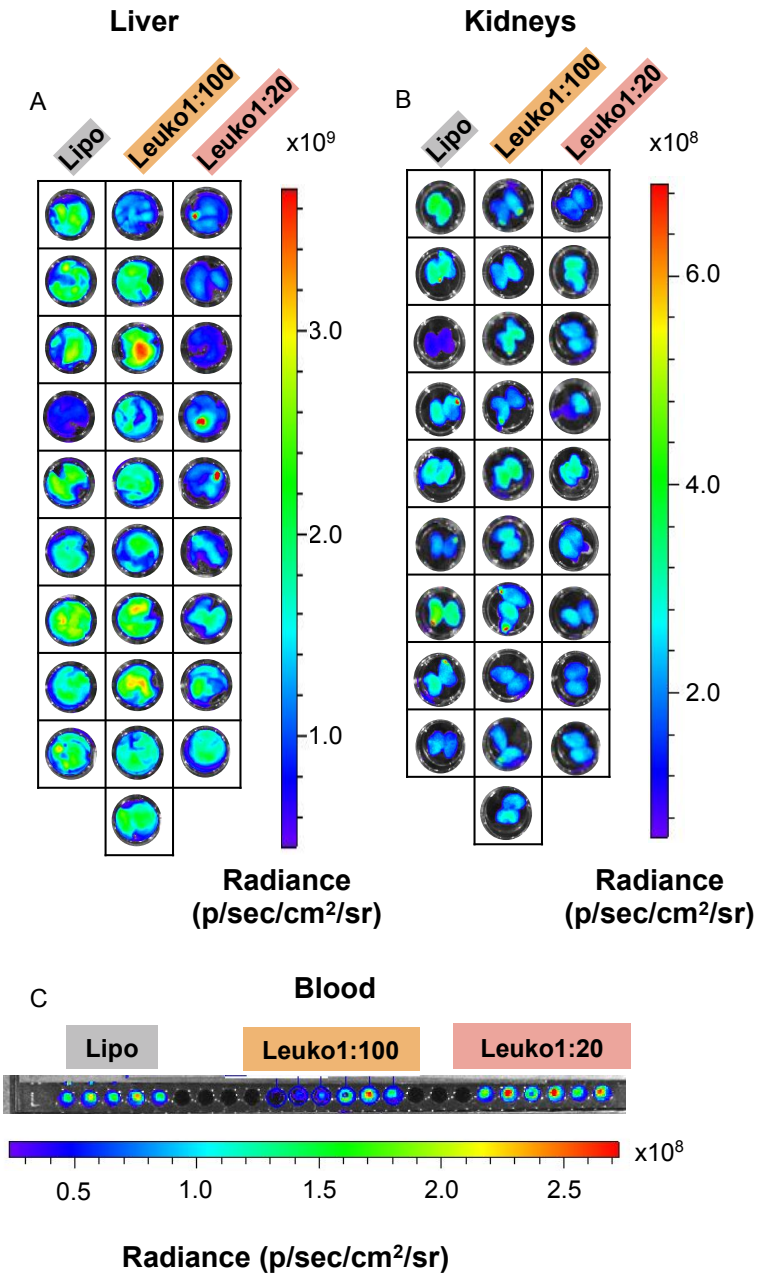

Fig. S16. Biomimetic NP accumulation in liver, kidneys and blood in LLI model after 8h
Ex vivo imaging of liver (A), kidneys (B) and blood (C) of the LLI model mice. Visual inspection revealed no major differences in NP accumulation in the liver and kidneys, while Leuko1:20 exhibited higher signal.

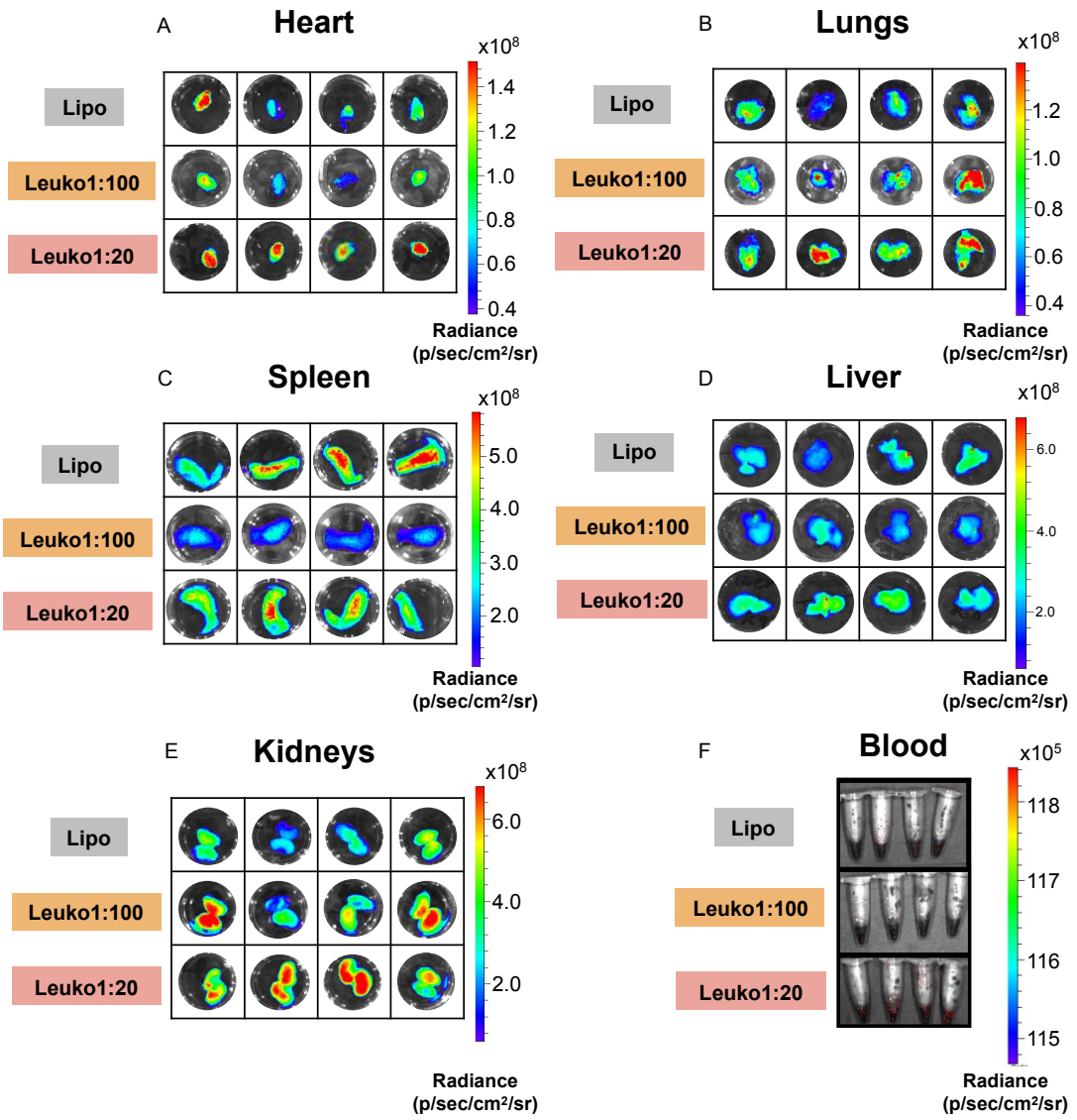

Fig. S17. Biomimetic NP accumulation in heart, lungs, spleen, liver, kidneys and blood of TNBC tumor-bearing mice after 24h

Ex vivo imaging of heart (A) and lungs (B), spleen (C), liver (D), kidneys (E) and blood (F).

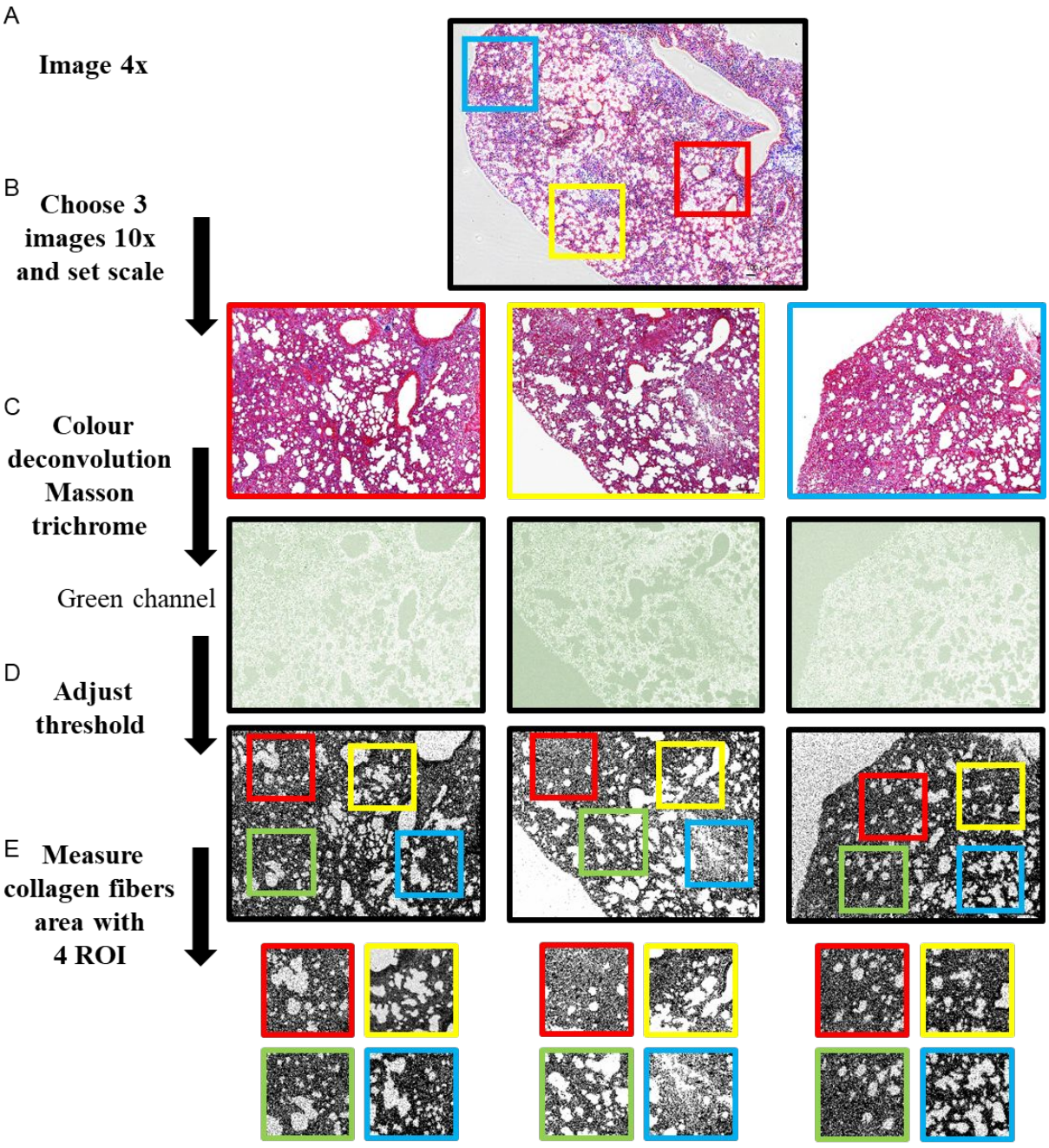
A
Image 4x
B
Choose 3 images 10x and set scale
C
Colour deconvolution Masson trichrome
Green channel
D
Adjust threshold
E
Measure collagen fibers area with 4 ROI

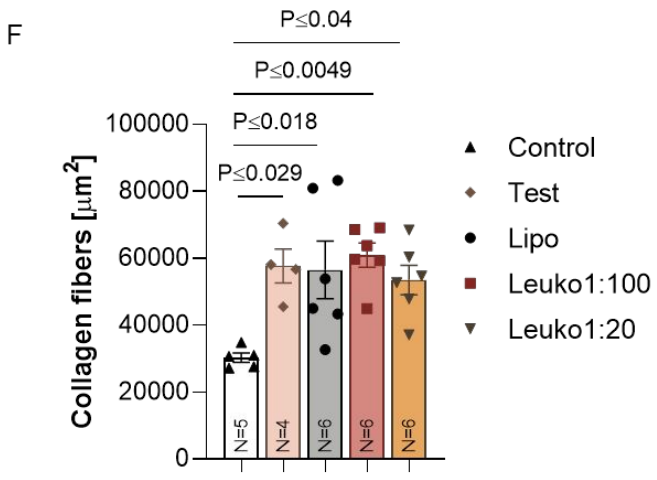
F
P≤0.04
P≤0.0049
P≤0.018
P≤0.029
Collagen fibers [µm²]
100000
80000
60000
40000
20000
0
N=5
N=4
N=6
N=6
N=6
Control
Test
Lipo
Leuko1:100
Leuko1:20

Fig. S18. Image analysis of collagen fibers workflow.
A) One representative 4x image was chosen B) For each image, three random 10x magnification images were chosen and the same scale was set for all (1.3pixel/μm). C) Masson's Trichrome color deconvolution plug-in was applied to each image and the green channel was chosen for the quantification of collagen fibers. D) The same threshold (min value was 235 and max value was 255) was applied to each image. E) A random ROI of the same size was generated, and quantification performed on 4 ROIs for each single image.[1] F) Quantification of collagen fibers revealed an increase in fibrosis following injection of LPS and no further increase observed in the NP injected mice.

References

1. Chen, Y.; Yu, Q.; Xu, C.-B., A Convenient Method for Quantifying Collagen Fibers in Atherosclerotic Lesions by Imagej Software. *Int J Clin Exp Med* **2017,** *10*, 14904-14910.